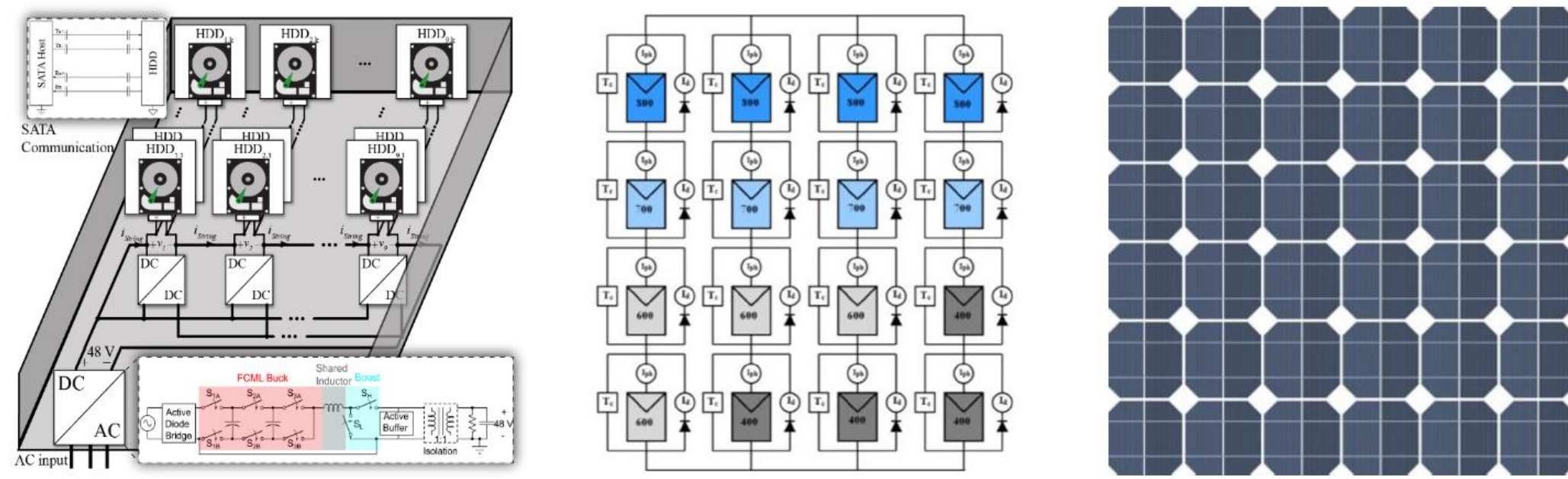


Towards Power FPGA: Architecture, Modeling and Control of Multiport Power Converters

Background & Motivation

- Future applications need multiport power converters



Server Racks Battery Systems Solar Cells

Fig. 1: Energy system with numerous modular power converters.

Circuit Topology for Multiport Converters

- Multi-stage v.s. single-stage multiport converters

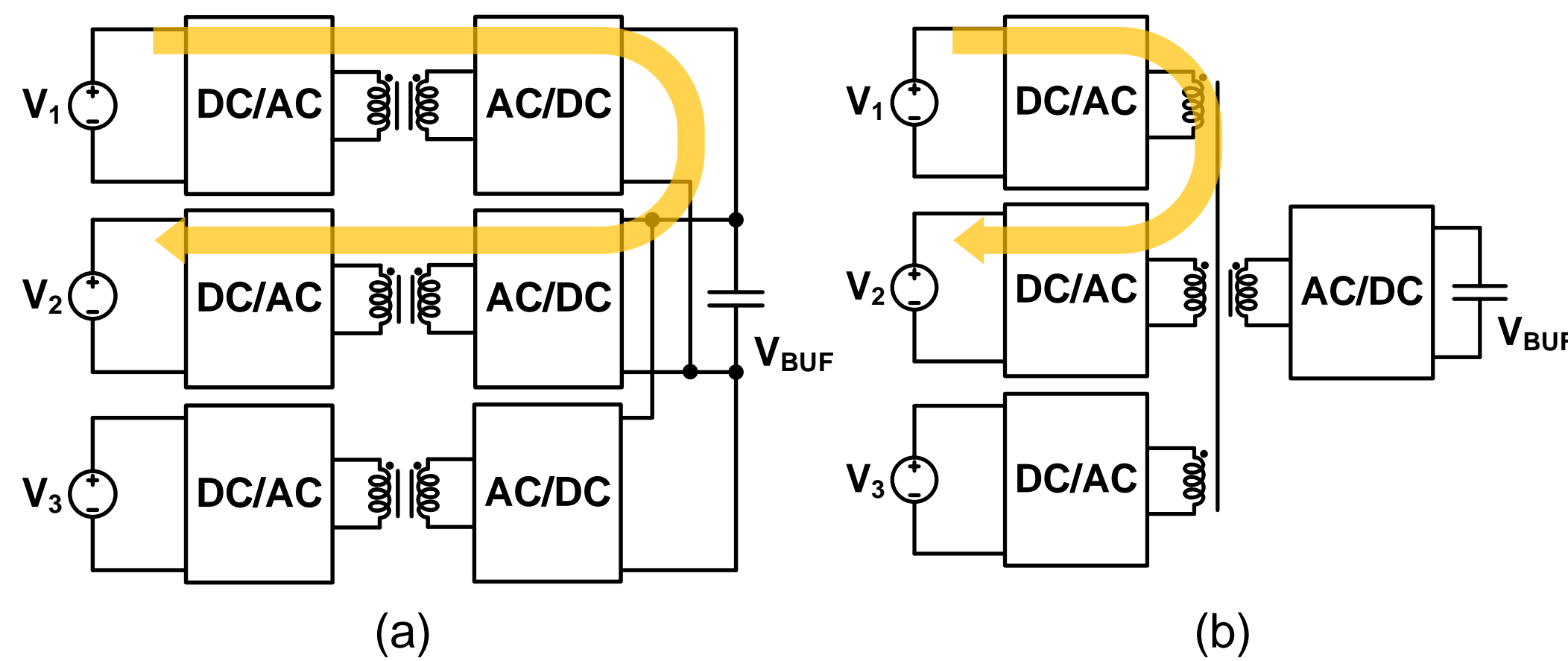


Fig. 2: (a) Multi-stage dc-ac-dc; (b) single-stage dc-ac-dc.

Table II: Advantages of the single-stage architecture.

Number of Devices	Multi-stage	Single-stage	Benefits
Dc-ac cells	6	4	33% size/cost reduction
Transformers	3	1	66% size/cost reduction
Dc-ac-dc stages	2	1	50% loss reduction

- Circuit topology of a generalized multiport power converter

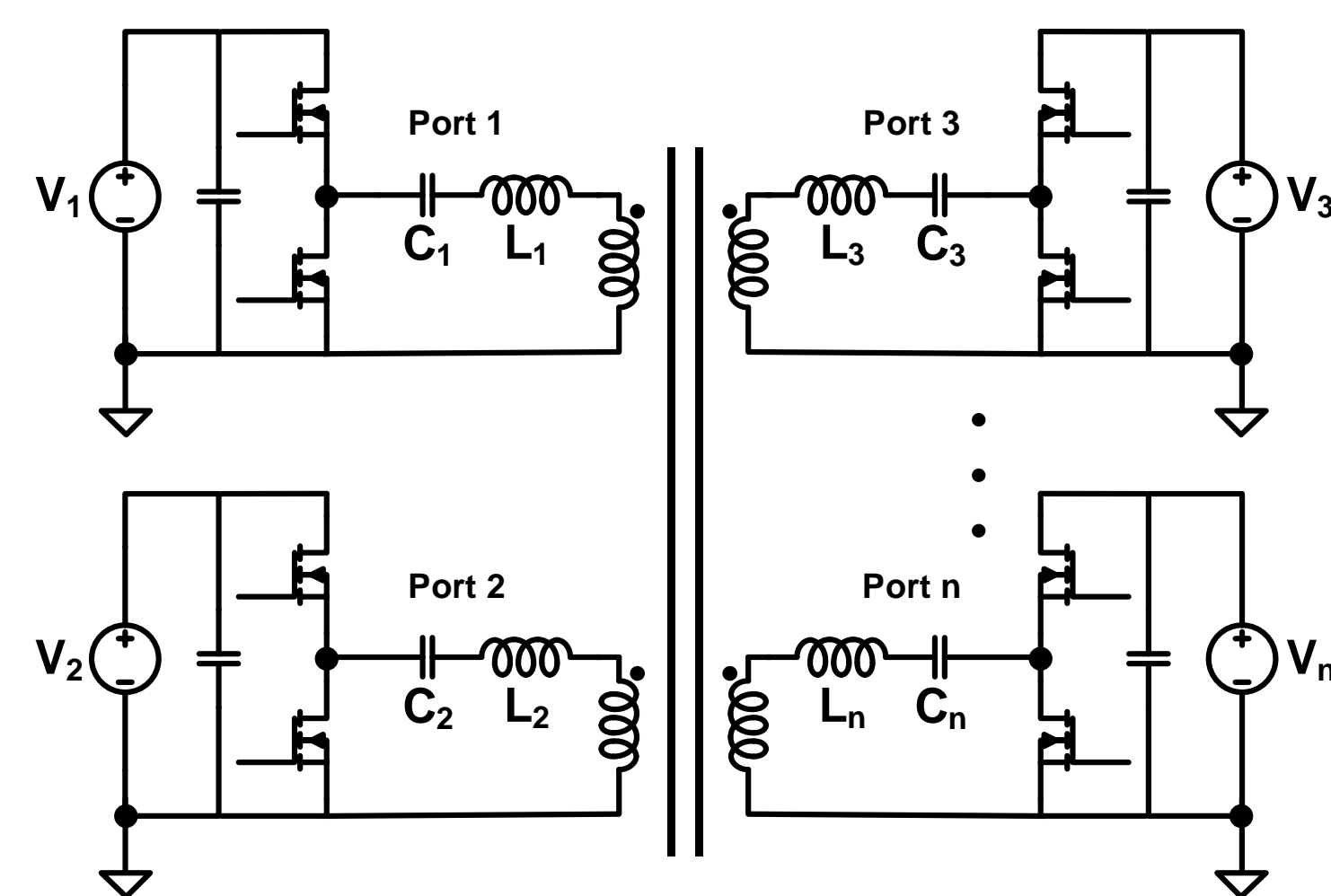


Fig. 3: Example topology of a multiport power converter.

Control Framework

- Equivalent circuit of the multi-winding transformer

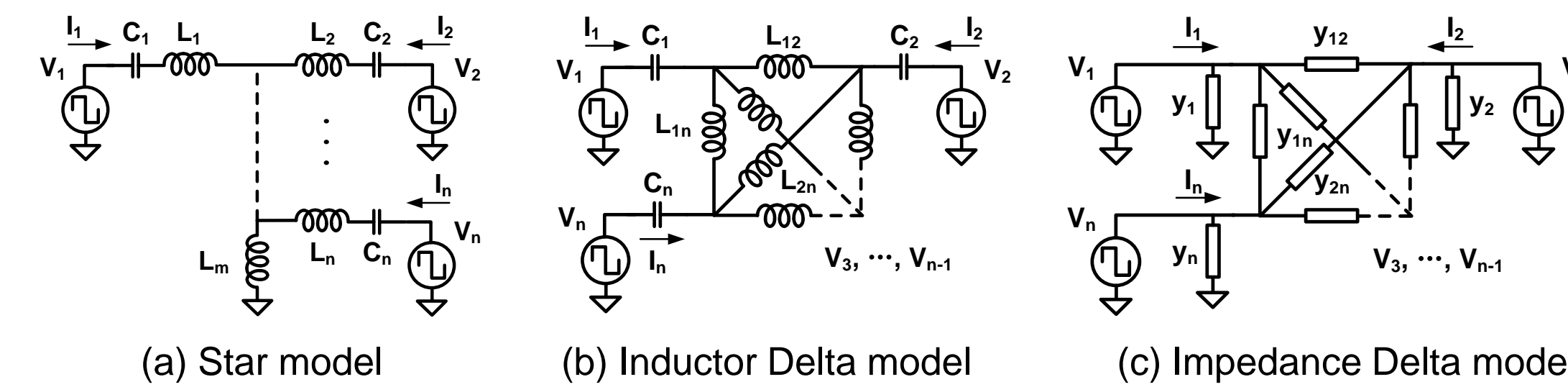


Fig. 4: Equivalent circuit.

- If C_i is very large: trapezoidal mode,

$$P_i = \sum_{k \neq i} \frac{V_i V_k}{\omega L_{ik}} \phi_{ik} \left(1 - \frac{\phi_{ik}}{\pi}\right)$$

- If C_i resonates with L_i : resonant mode,

$$P_i = \frac{8}{\pi^2} \sum_{k=1}^n V_i V_k (G_{ik} \cos \phi_{ik} + B_{ik} \sin \phi_{ik})$$

$$\begin{cases} P_1 \\ P_2 \\ \vdots \\ P_{n-1} \end{cases} = f: R^{n-1} \rightarrow R^{n-1} \begin{cases} \phi_1 \\ \phi_2 \\ \vdots \\ \phi_{n-1} \end{cases}$$

- Control framework

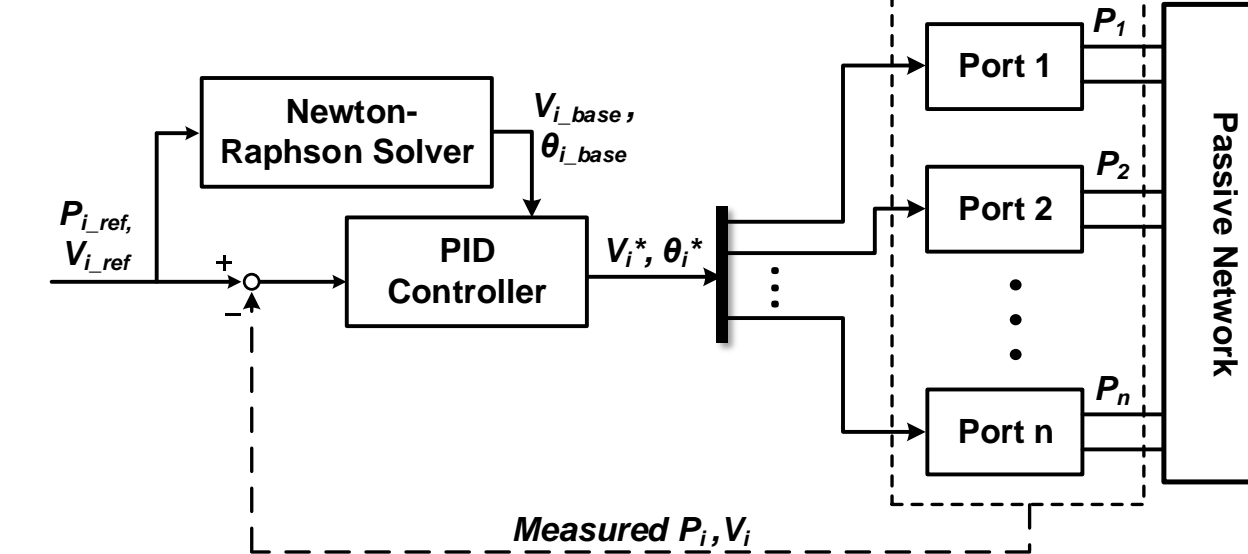


Fig. 5: Control framework.

- Solver tool in Github: <https://github.com/PingWang3741/Multiport-Power-Converter.git>

Power Rating & Convergence Analysis

- Power rating of the multiport converters

- Maximal and minimal power in trapezoidal mode

$$P_{i,max} = \frac{\pi}{4} \sum_{k \neq i} \frac{V_i V_k}{\omega L_{ik}}$$

$$P_{i,min} = -\frac{\pi}{4} \sum_{k \neq i} \frac{V_i V_k}{\omega L_{ik}}$$

- Maximal and minimal power in resonant mode

$$a = -\frac{8}{\pi^2} \sum_{k \neq i} G_{ik} \quad b = \frac{8}{\pi^2} \sum_{k \neq i} V_{k,max} \sqrt{G_{ik}^2 + B_{ik}^2}$$

$$P_{max} = \begin{cases} \frac{8}{\pi^2} \sum_{k \neq i} (V_{k,max} \sqrt{G_{ik}^2 + B_{ik}^2} - V_{i,max} G_{ik}) V_{i,max} & a \geq 0 \\ \frac{8}{\pi^2} \frac{(\sum_{k \neq i} V_{k,max} \sqrt{G_{ik}^2 + B_{ik}^2})^2}{4 \sum_{k \neq i} G_{ik}} & a < 0 \text{ \& } -\frac{b}{2a} \leq V_{i,max} \\ \frac{8}{\pi^2} \sum_{k \neq i} (V_{k,max} \sqrt{G_{ik}^2 + B_{ik}^2} - V_{i,max} G_{ik}) V_{i,max} & a < 0 \text{ \& } -\frac{b}{2a} > V_{i,max} \end{cases}$$

$$P_{min} = \begin{cases} -\frac{8}{\pi^2} \sum_{k \neq i} (V_{k,max} \sqrt{G_{ik}^2 + B_{ik}^2} + V_{i,max} G_{ik}) V_{i,max} & a < 0 \\ \frac{8}{\pi^2} \frac{(\sum_{k \neq i} V_{k,max} \sqrt{G_{ik}^2 + B_{ik}^2})^2}{4 \sum_{k \neq i} G_{ik}} & a \geq 0 \text{ \& } \frac{b}{2a} \leq V_{i,max} \\ -\frac{8}{\pi^2} \sum_{k \neq i} (V_{k,max} \sqrt{G_{ik}^2 + B_{ik}^2} + V_{i,max} G_{ik}) V_{i,max} & a \geq 0 \text{ \& } \frac{b}{2a} > V_{i,max} \end{cases}$$

- Convergence analysis

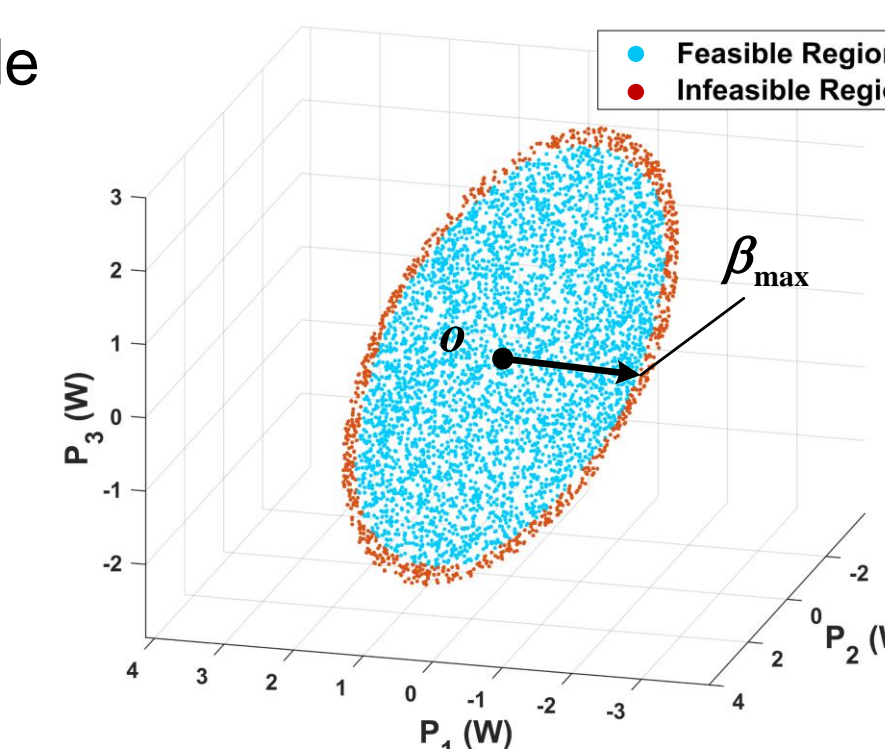


Fig. 6: Power rating analysis.

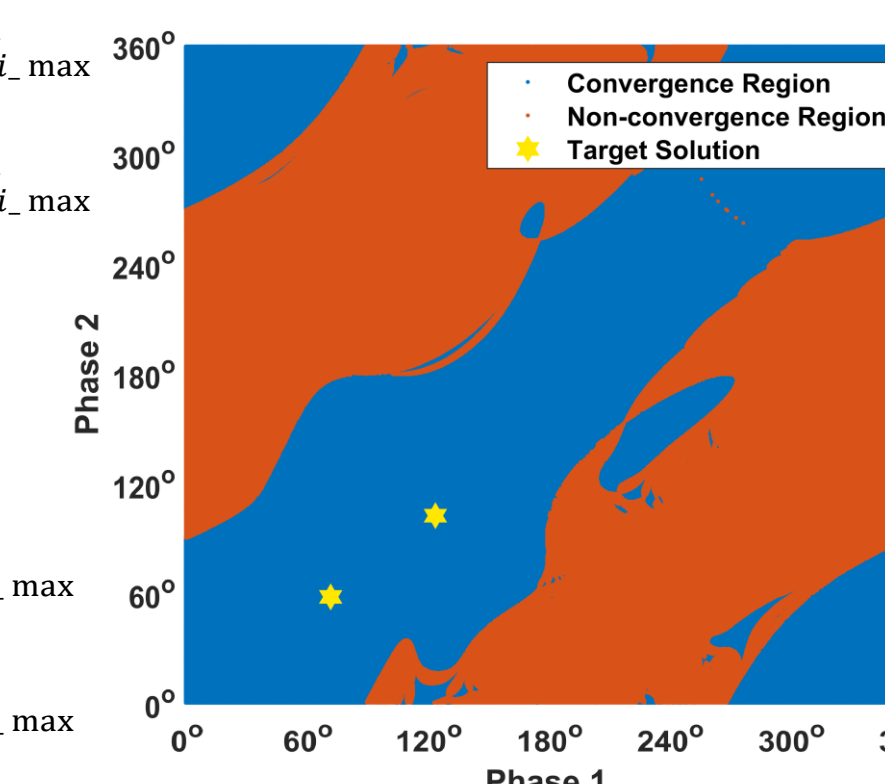
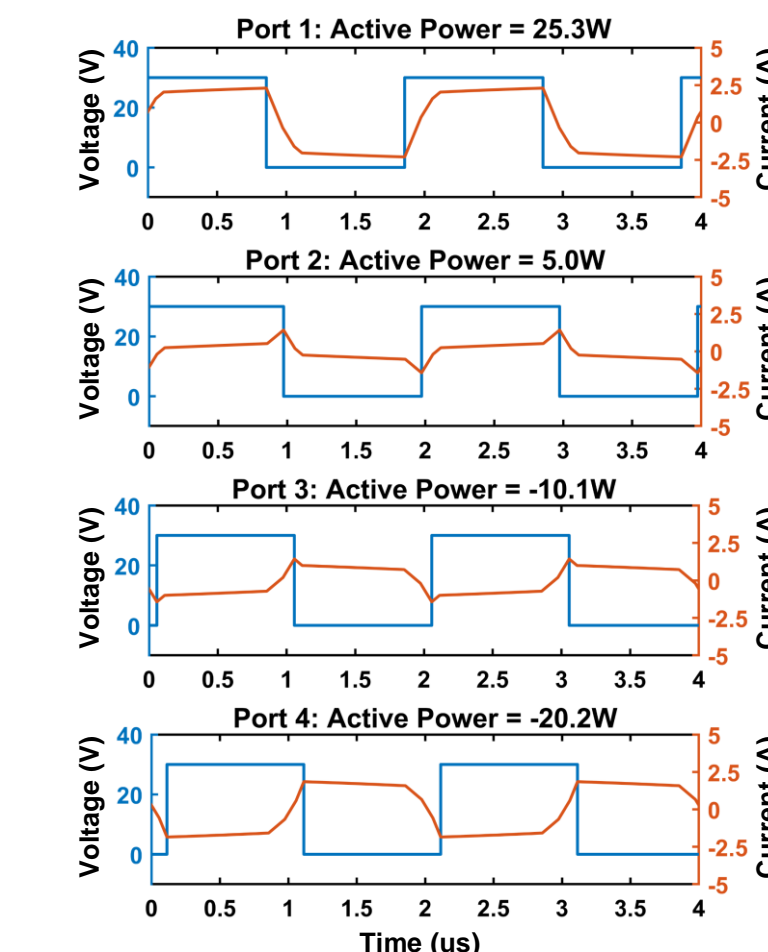


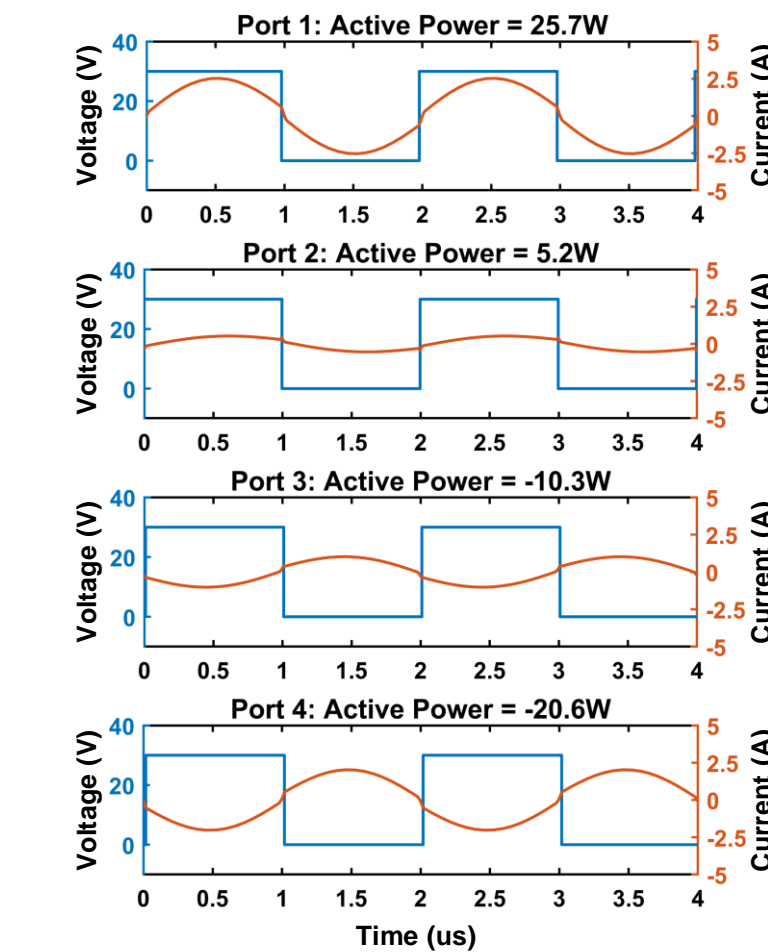
Fig. 7: Convergence analysis.

Simulation Results

- Simulation with 4 ports



(a) Trapezoidal



(b) Sinusoidal

Fig. 8: Simulated waveforms.

- Simulation with 100 ports

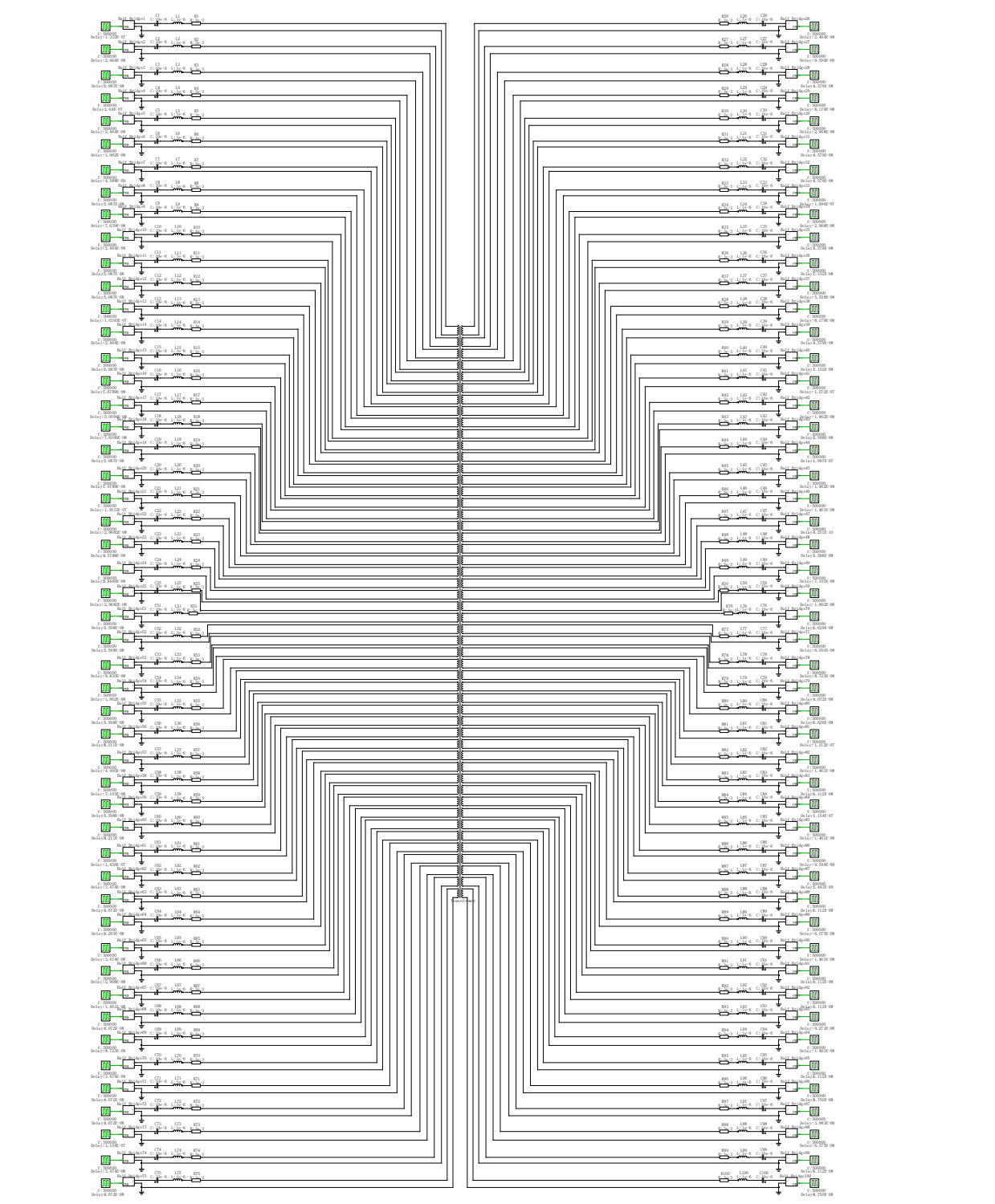


Fig. 9: 100-port "Power FPGA".

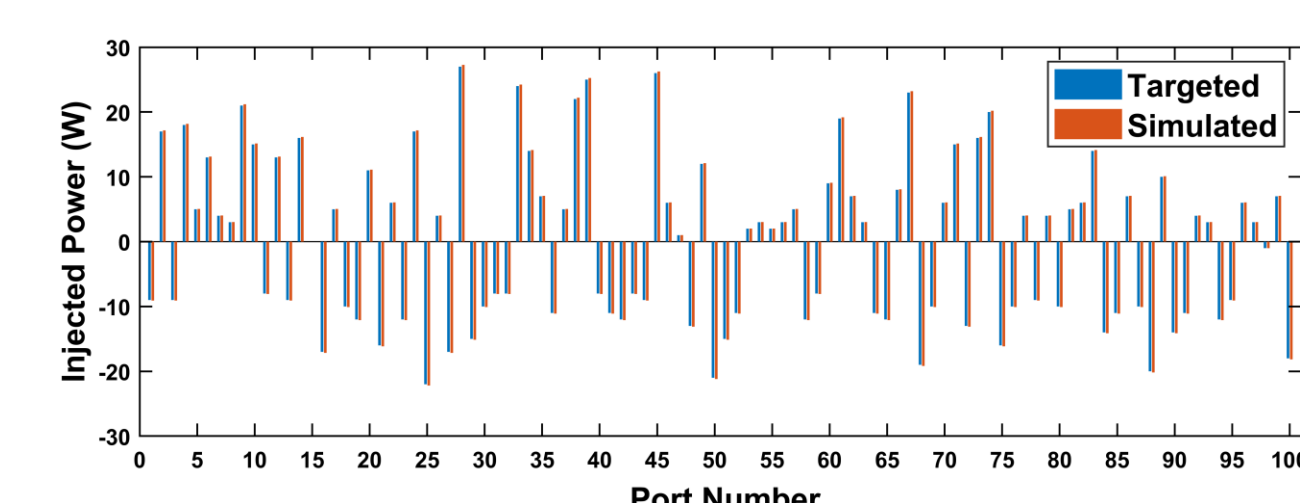


Fig. 10: 100-port power programming.

Experimental Results

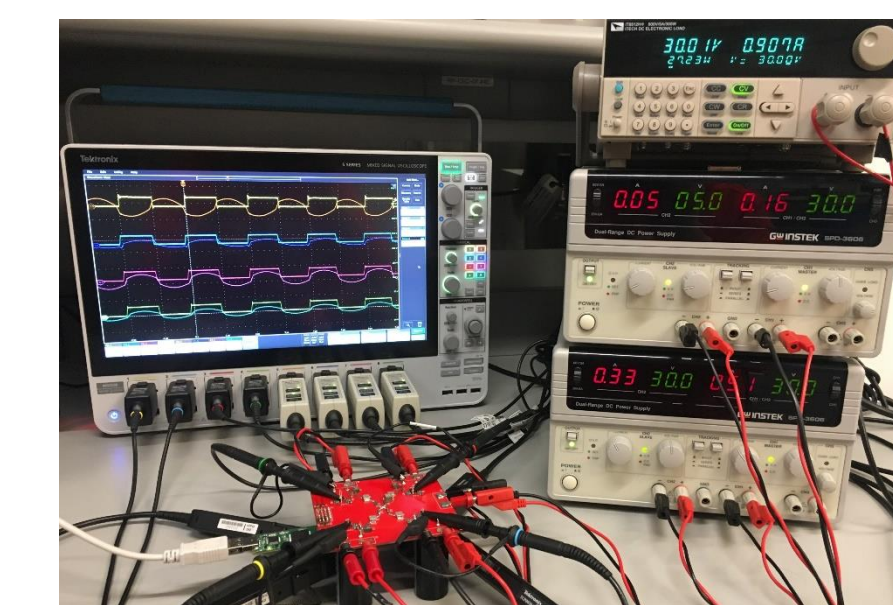


Fig. 11: Experimental setup.

- Three example cases

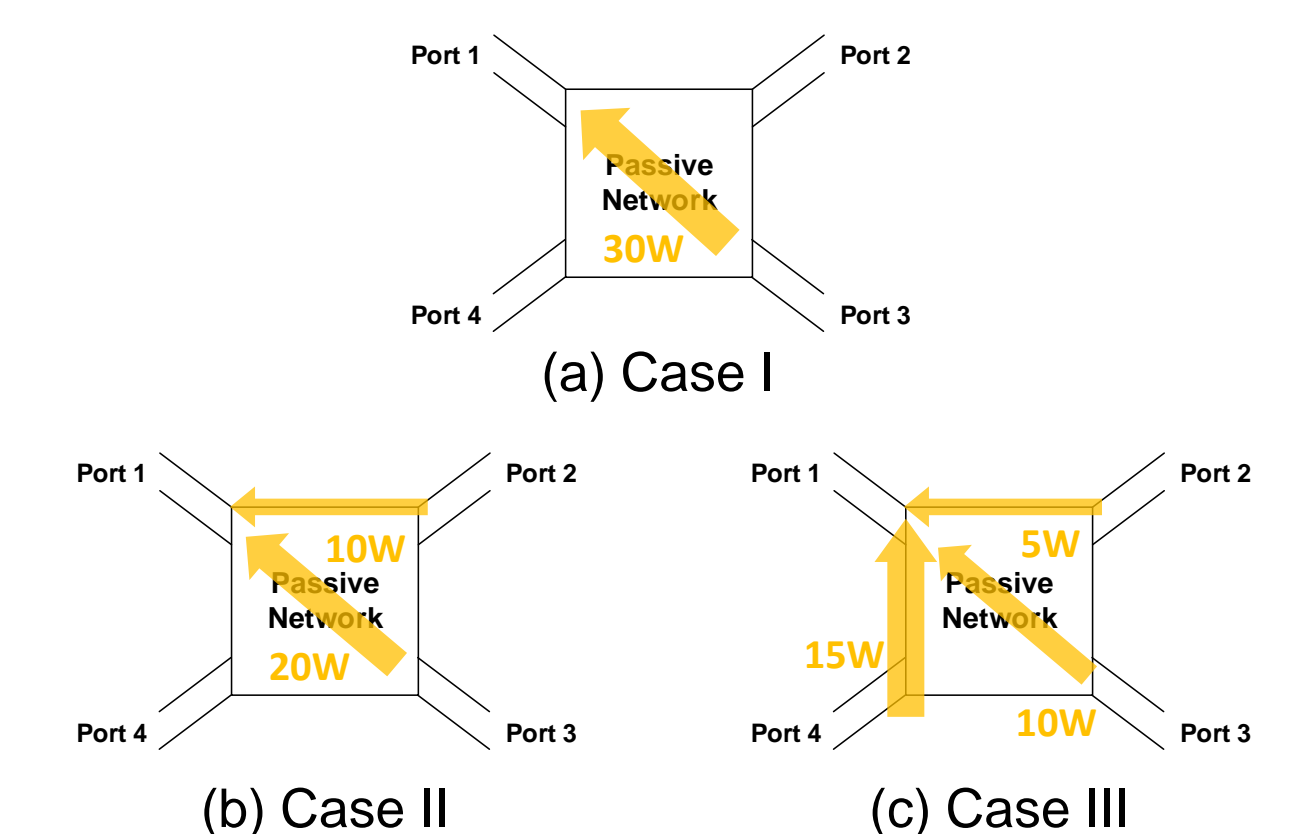


Fig. 13: Three typical power flow.

- Experimental results of three cases

Table II: Simulation & experimental results.

	Power (w)	Port 1	Port 2	Port 3	Port 4
Case I	Target	-30.00	0.00	30.00	0.00
	Trapezoidal	-27.25	0.9	32.4	0.6
Case II	Target	-30.00	10.00	20.00	0.00
	Trapezoidal	-27.67	10.8	21.3	0.6
Case III	Target	-30.00	5.00	10.00	15.00
	Trapezoidal	-27.83	5.1	11.4	15.6
	Resonant	-27.23	4.80	9.90	15.30

Fig. 12: Experimental waveforms.